

Magnetic Design of a 20 mm Hybrid Undulator for CLS

6.2.25.4 Rev. 0

Date: 2003-01-16

Copyright 2003, Canadian Light Source Inc. This document is the property of Canadian Light Source Inc. (CLSI). No exploitation or transfer of any information contained herein is permitted in the absence of an agreement with CLSI, and neither the document nor any such information may be released without the written consent of CLSI.

Canadian Light Source Inc.
101 Perimeter Road
University of Saskatchewan
Saskatoon, Saskatchewan Canada

Signature

Date

Original on File – Signed by:

Author

Ingvar Blomqvist

Reviewer #1

Les Dallin

Reviewer #2

Pawel Grochulski

Reviewer #3

Dan Lowe

Approver

Mark de Jong

BLANK PAGE

REVISION HISTORY

<i>Revision</i>	<i>Date</i>	<i>Description</i>	<i>Author</i>
A	02-01-10	Original Draft	Ingvar Blomqvist
B	03-01-16	Comments included	Ingvar Blomqvist
0	03-01-16	Issued for use	Ingvar Blomqvist

BLANK PAGE

TABLE OF CONTENTS

1.0	ABSTRACT/SUMMARY	1
2.0	INTRODUCTION	1
2.1	PURPOSE	1
2.2	SCOPE	1
2.3	DESIGN CALCULATIONS	1
2.4	LIMITS ON FIELD INTEGRALS AND INTEGRATED MULTIPOLES	1
3.0	MAGNETIC PROPERTIES	2
3.1	SELECTION OF MATERIAL AND PERIOD LENGTH	2
3.2	MAGNETIC LAYOUT	3
3.3	MAGNETIC FLUX DENSITIES AND FIELD INTEGRALS	5
3.4	CALCULATION OF DE-MAGNETIZING FIELDS	11
3.5	EFFECTS ON THE STORED ELECTRON BEAM	13
3.6	PERMANENT MAGNET MATERIAL, MANUFACTURING AND QUALITY CONTROL	14
3.7	MOUNTING OF THE MAGNET ASSEMBLIES	15
3.8	CORRECTION COILS	15
3.9	SUMMARY	16
4.0	REFERENCES	17

BLANK PAGE

1.0 ABSTRACT/SUMMARY

The report gives the details of the magnetic design for a 20 mm period hybrid in-vacuum undulator covering the photon energy range from 6 keV to 18 keV. The undulator will operate with a minimum gap of 5 mm. The design has 157 full size pole pairs and 2 thin end pole pairs. A permanent magnet material has been chosen that is resistant to radiation damage and allows baking of the undulator vacuum system at high temperature. It meets all requirements on the field integrals and integrated multipoles with the help of magic fingers. The de-magnetizing fields and the effect on the stored beam have been calculated.

2.0 INTRODUCTION

2.1 PURPOSE

This conceptual design report describes the magnetic design of a 20 mm period hybrid undulator covering the photon energy range from 6 keV to 18 keV.

2.2 SCOPE

This report covers only the magnetic design; the mechanical structure will be designed and manufactured by an outside company using existing in-vacuum undulator structures at ESRF and SPring-8 as models.

2.3 DESIGN CALCULATIONS

The design calculations were made with RADIA [1], using a 13-pole model undulator. RADIA uses a coordinate system where the y-axis is the longitudinal axis, the z-axis the vertical axis and the x-axis the transverse axis, and this system is used in the figures in this report.

The magnetic field distribution is not uniform over the magnet blocks and poles, and they must be subdivided into smaller elements. The subdivision shown in the pictures of the poles and magnet blocks has been used in the calculations. The iron poles must have a rather fine subdivision, for the permanent magnet blocks the subdivision can be considerably coarser.

The relative permeability of 1.06 parallel to and 1.17 perpendicular to the easy axis of the blocks is included in the calculations. For the poles the material function RadMatAFK502[] in RADIA has been used. This describes a Vanadium Permendur material with a saturation magnetization of 2.35 T.

2.4 LIMITS ON FIELD INTEGRALS AND INTEGRATED MULTIPOLES

Limits must be placed on the field integrals and the integrated multipoles of the undulator to avoid disturbing the stored electron beam. The limits for the first and second field integrals on the undulator center line are

$$\begin{aligned} |I_1^x| = |I_1^z| &< 50 \cdot 10^{-6} \text{ T}\cdot\text{m} = 5 \text{ } \mu\text{rad} \text{ for a 2.9 GeV beam} \\ |I_2^x| = |I_2^z| &< 50 \cdot 10^{-6} \text{ T}\cdot\text{m}^2 = 5 \text{ } \mu\text{m} \text{ for a 2.9 GeV beam} \end{aligned}$$

The limits on the integrated multipoles are given in Table 1. The limits are valid in the interval $(-10 \text{ mm} < x < 10 \text{ mm})$. The limits on integrals and integrated multipoles are valid for all gap sizes.

Table1. Limits on the integrated multipole components.

Integrated Multipole	Horizontal	Vertical
Quadrupole	$< 5 \cdot 10^{-3} \text{ T}$	$< 5 \cdot 10^{-3} \text{ T}$
Sextupole	$< 0.6 \text{ T/m}$	$< 0.6 \text{ T/m}$
Octupole	$< 100 \text{ T/m}^2$	$< 100 \text{ T/m}^2$

3.0 MAGNETIC PROPERTIES

3.1 SELECTION OF MATERIAL AND PERIOD LENGTH

An undulator capable of delivering 18 keV light with a 2.9 GeV incident electron energy must have a small period but also a reasonably high k as we need to use harmonics as high as 9th and 11th to reach 18 keV. A high k means high peak flux density, which for small period lengths means small minimum gap. The properties of the CLS electron beam should allow a minimum gap of 5 mm.

To operate at a magnetic gap of 5 mm we need to place the magnet assemblies inside the electron beam vacuum chamber, which means we need an in-vacuum undulator. This puts additional requirements on the permanent magnet material. We must be able to bake the magnet assemblies at high temperature to achieve the UHV vacuum needed in the storage ring, and the magnet blocks must be coated with an UHV-compatible material.

At 5 mm gap there is a chance the magnet assemblies will be hit by electrons far out on the tails of the distribution. These electrons will create bremsstrahlung photons and fast neutrons, which will interact with the permanent magnet material.

It is well known that $\text{Sm}_2\text{Co}_{17}$ permanent magnet material is less sensitive to radiation damage compared to the more common NdFeB. The $\text{Sm}_2\text{Co}_{17}$ material also has a much lower temperature coefficient for the intrinsic coercivity (H_{CJ}) compared to the NdFeB material, which makes it more suitable for baking at high temperatures. We have therefore decided to use $\text{Sm}_2\text{Co}_{17}$ for the magnet blocks in the undulator.

However, the $\text{Sm}_2\text{Co}_{17}$ material has a lower remanence (B_r) compared to the more common NdFeB material. We can partly compensate the lower B_r by using a hybrid layout for the undulator, where the poles are made from ferromagnetic material. The high saturation magnetization for iron compared with permanent magnet material, $> 2 \text{ T}$ compared to about 1.2 T, allows us to use thinner poles, which increases the amount of permanent magnet material, and we can recover some of the loss in peak flux density. The draw back is the non-linear relative permeability of iron, which introduces non-linear behavior in the field integrals. The iron poles also pick up and amplify the earth's field and stray magnetic fields, which also affects the field integrals.

To get the highest possible peak flux density we chose Vanadium Permendur material with equal amount of Co and Fe and about 2% V. The material has a saturation magnetization of 2.35 T compared to 2.1 T for pure Fe. The disadvantage is the material is very hard and brittle and difficult to machine and therefore rather expensive.

The length of the undulator will be decided when the support structure with vacuum chamber is designed. It is estimated to be 1600 mm, which would allow two ESRF-type undulators to be installed in the same straight section.

We have found a period length of 20 mm to give the best compromise between contrasting requirements of a continuous tuning curve with maximum brilliance in the specified photon energy

range and keeping the required maximum harmonic number as small as possible. The estimated brilliance for the undulator with the CLS electron beam parameters for year 2008 [2] has been calculated using SRW [3], and is shown in Figure 1. We need harmonics 3 to 11 to cover the specified photon range.

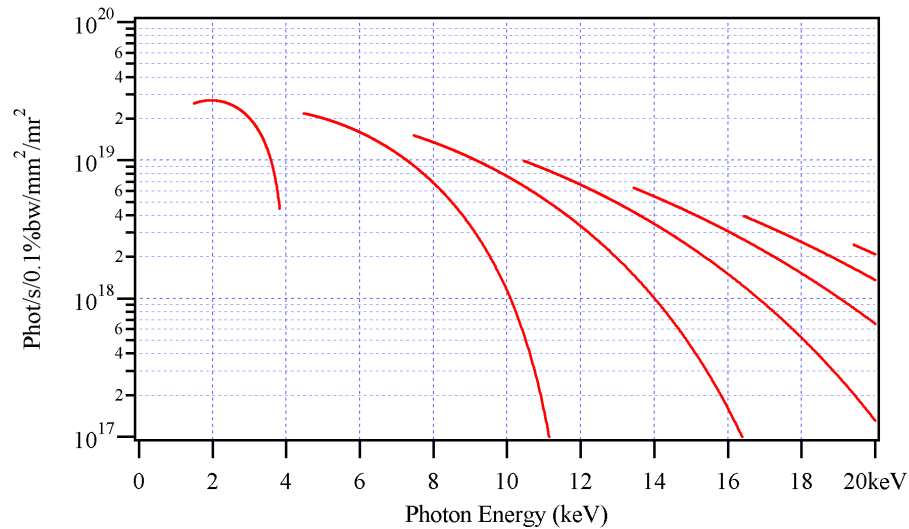


Figure 1. Estimated brilliance for the 1.6 m long 20 mm period in-vacuum undulator using the year 2008 beam parameters. The calculation is for a perfect undulator with no errors.

3.2 MAGNETIC LAYOUT

The layout of the full size poles and magnet blocks are shown in Figures 2 and 3. The poles are 2.5 mm thick, 22 mm high and 33 mm wide. A 3 x 3 mm² ear is sticking out on each side to secure the pole in the pole holder. There is a 4 mm deep, 45° cut at the pole bottom to increase the flux density in the middle of the pole and improve the transverse roll-off. As mentioned in the previous section the poles will be made of Vanadium Permendur with a saturation magnetization of 2.35 T. This is a sintered material, and the poles must be coated to be compatible with UHV requirements. A suitable coating might be a few μm of Ag, which also would reduce the friction between the poles and the magnet blocks.

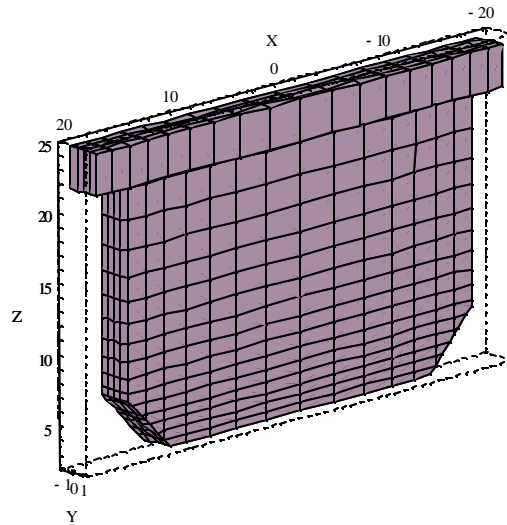


Figure 2. Full size pole

The magnet blocks are 7.5 mm thick, 30 mm high and 50 mm wide. There is a 5 mm deep, 45° cut at the corners to clamp the blocks in the holders. The blocks are made from $\text{Sm}_2\text{Co}_{17}$ and must be coated with TiN or Ni to be HUV compatible.

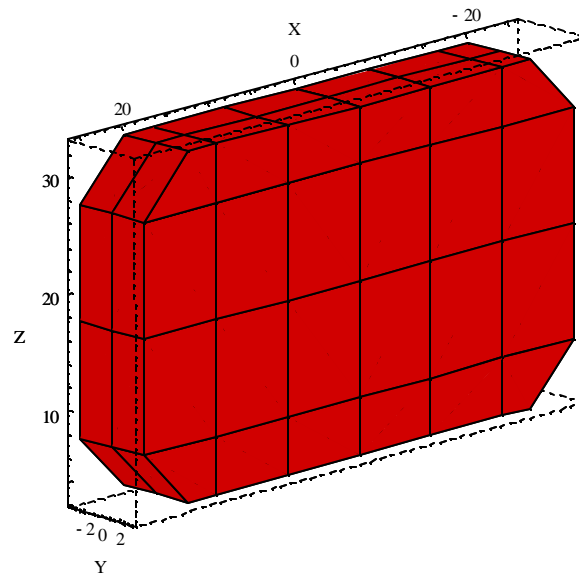


Figure 3. Full size magnet block.

Figure 4 shows the lower part of the 13 pole model undulator. The end sections consists of a half thickness pole surrounded by magnet blocks with their thickness reduced by 20% and 66% respectively [4]. There is a 2.7 mm space between the thin pole and the surrounding blocks. The

end section parameters have been optimized to minimize the variation of the field integrals as function of the undulator gap size.

The finite width of the poles introduces high order Fourier components in the field integrals, and we use small blocks of permanent magnet material, 2 mm diameter and 2 mm high, to correct the first integral as a function of x . The number of blocks needed and their positions for the model undulator is shown in Figure 4.

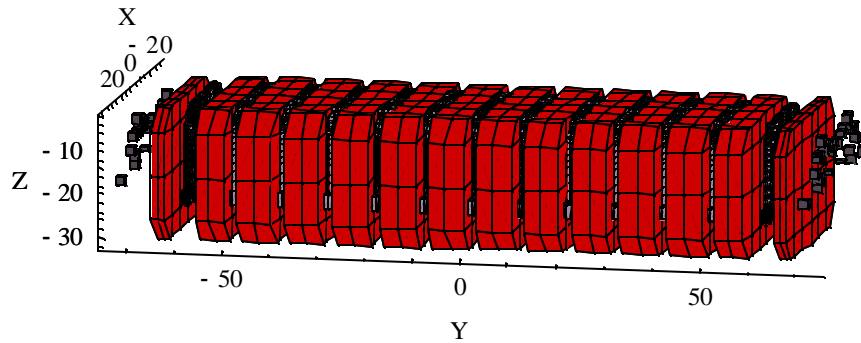


Figure 4. The lower half of the model undulator.

3.3 MAGNETIC FLUX DENSITIES AND FIELD INTEGRALS

The flux density distribution on the magnetic mid plane at minimum gap is shown in Figure 5, and the flux density on the undulator centerline at minimum gap in Figure 6. The thin poles introduces higher order Fourier components in the flux density distribution, the peak effective flux density is lower than the peak flux density. The photon energy is 1.488 keV, and the magnetic force 9.5 kN.

The vertical first integral in the interval $-50 \text{ mm} < x < 50 \text{ mm}$ is shown in Figure 7, the horizontal first and second integrals are zero due to symmetry. The orbits for a 2.9 GeV electron on the mid plane for $x = 0, 2, 4, 6, 8$ and 10 mm are shown in Figure 8. The oscillation amplitude is about 1 μm . The end sections have very small horizontal offsets inside the undulator. The vertical second integral is small as can be expected from the very small first integral.

The peak effective flux density, the photon energy, the vertical first and second integrals and the magnetic force as function of the undulator gap are shown in Figures 9-13. The second integral has been extrapolated to the length of the full size undulator. The field integrals are well within specifications for all gaps.

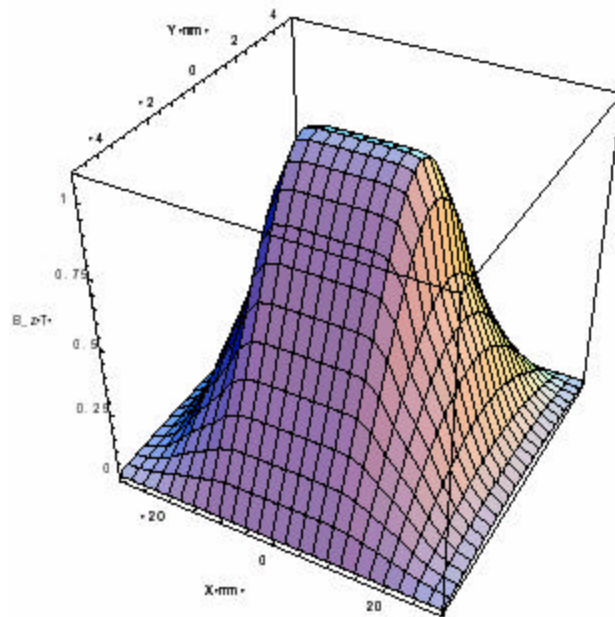


Figure 5. The magnetic flux density distribution on the magnetic mid plane.

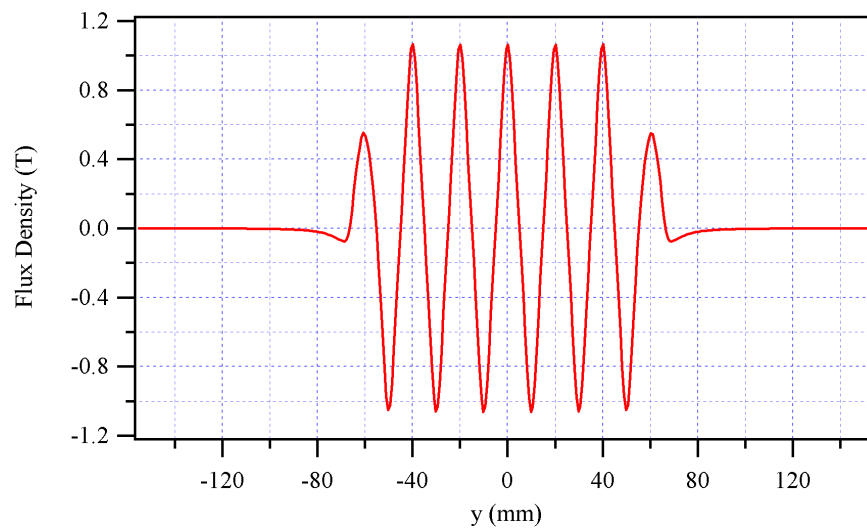


Figure 6. The magnetic flux density on the undulator center line at minimum gap.

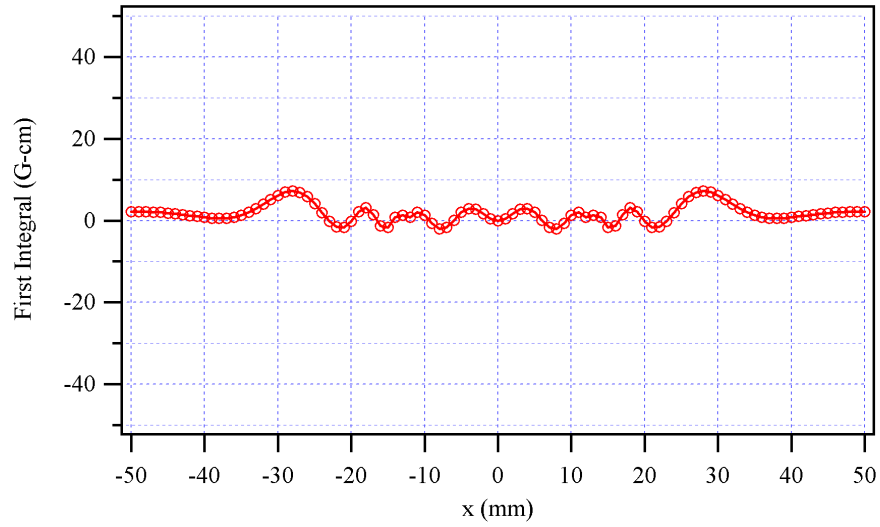
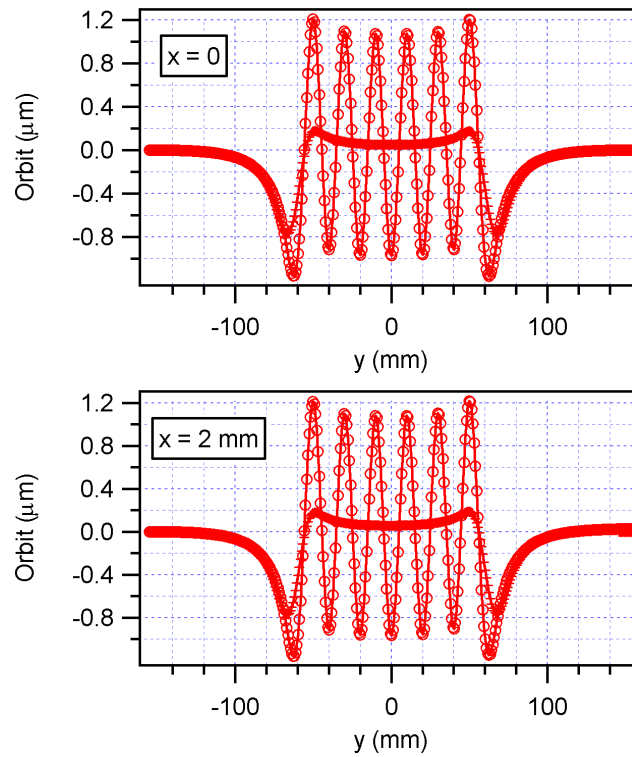


Figure 7. The vertical first integral at minimum gap as a function of x.



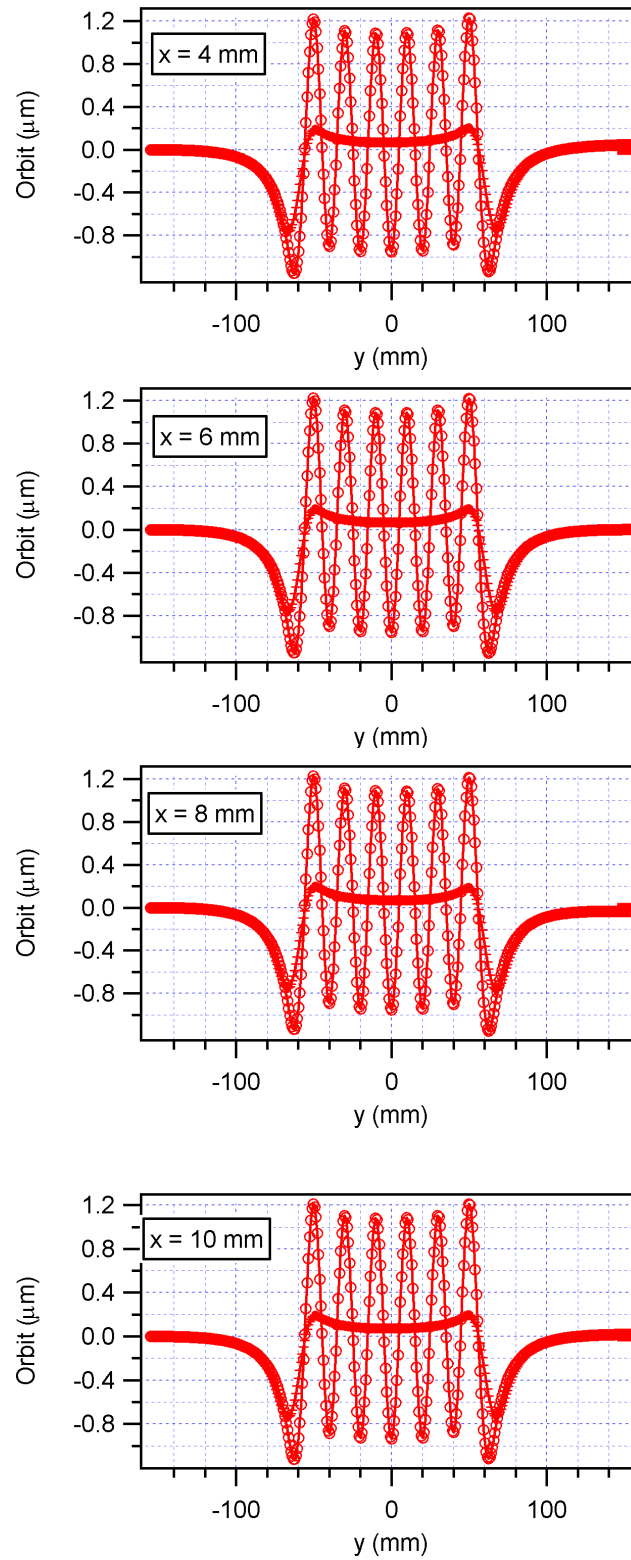


Figure 8. The orbits for a 2.9 GeV electron through the undulator at minimum gap. The smooth horizontal line is the electron orbit averaged over one period to eliminate the oscillatory behavior.

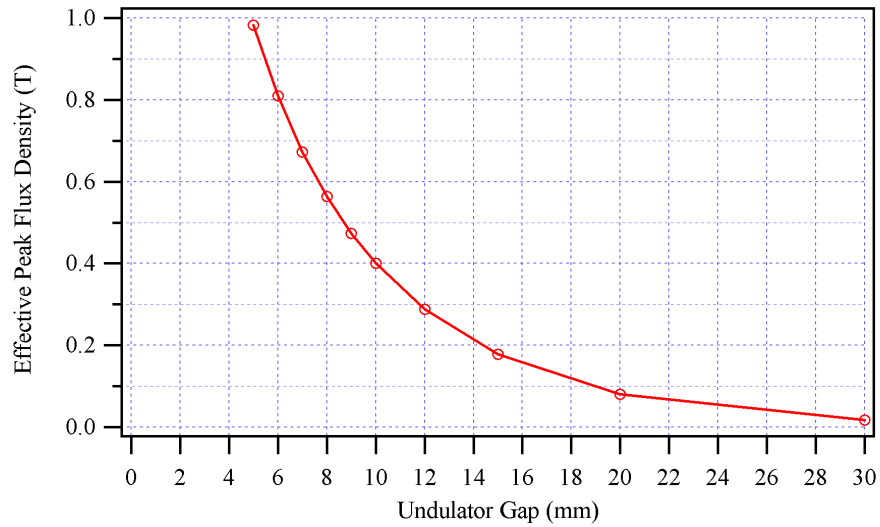


Figure 9. The peak effective flux density as a function of the undulator gap.

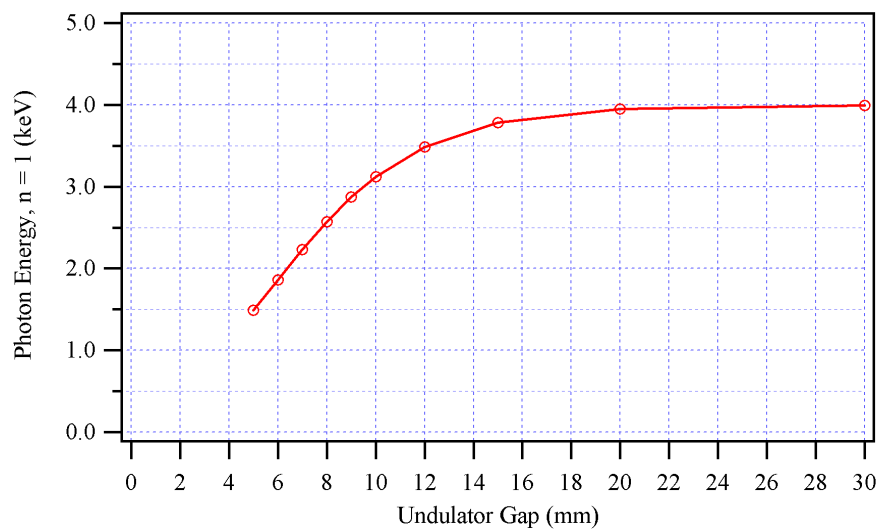


Figure 10. The photon energy for the first harmonics peak as a function of the undulator gap.

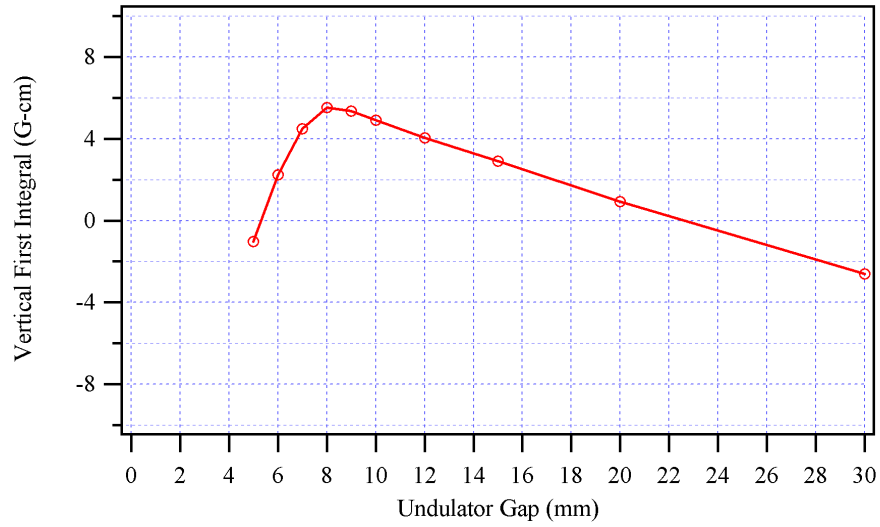


Figure 11. The vertical first integral as a function of the undulator gap.

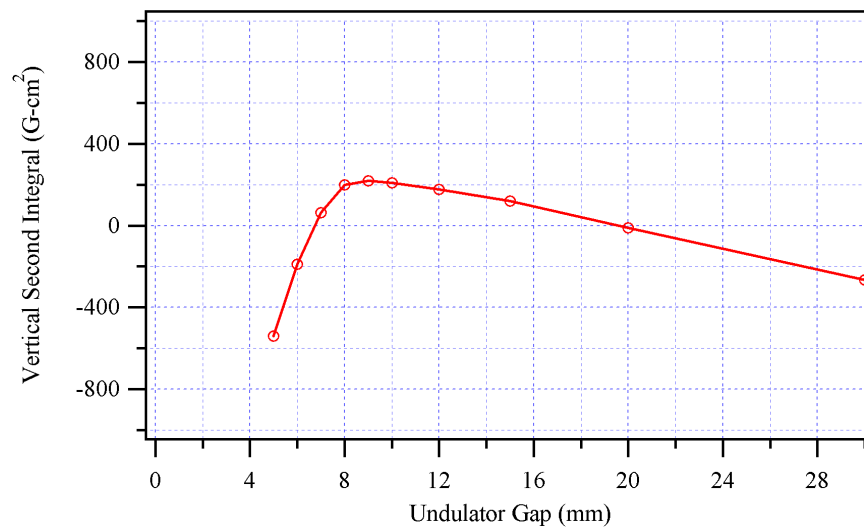


Figure 12. The vertical second integral as a function of the undulator gap.

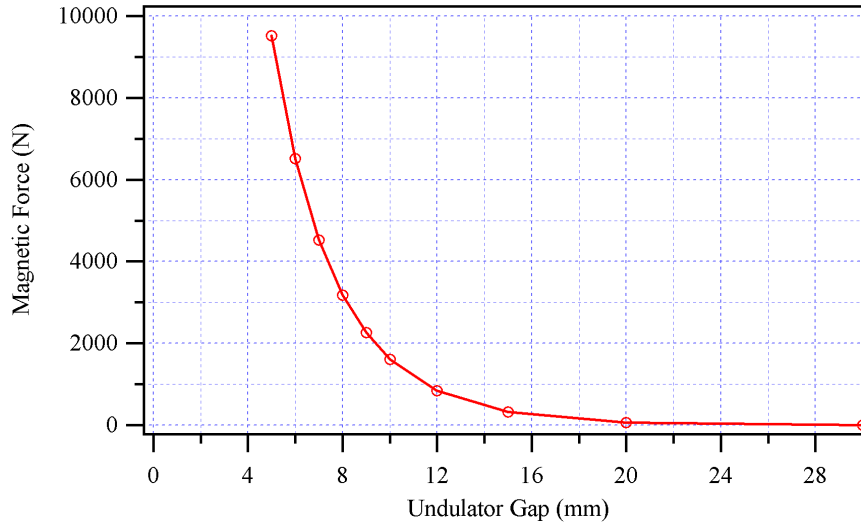


Figure 13. The magnetic force as a function of the undulator gap.

3.4 CALCULATION OF THE DE-MAGNETIZING FIELDS

The de-magnetizing fields have been calculated for the worst-case scenario, which is for a single magnet assembly and for the blocks in the middle of the undulator. If the de-magnetizing field in some part of a magnet block is larger than the intrinsic coercivity for the material, the polarization of that part of the block will be reversed. This might give large effects in the field integrals, which cannot be shimmed away. H_{cJ} has a negative temperature coefficient, and it is important to consider the highest temperature the undulator will be exposed to. This is especially important for an in-vacuum undulator, which needs to be baked at high temperatures.

The demagnetizing field in the horizontal blocks is shown in Figures 14 and 15. The largest value is 14.5 kOe = 1155 kA/m at the air gap, where the pole ends.

The data used in the design calculations are the catalogue data for VACOMAX 225 HR from Vakuumschmelze GmbH in Germany, but other manufacturers have similar materials. The 225 HR has a minimum remanence of 1.03 T and a minimum intrinsic coercivity of 20 kOe at 20°C. The temperature coefficients are $-0.035\%/^{\circ}\text{C}$ for the remanence and $-0.19\%/^{\circ}\text{C}$ for the intrinsic coercivity. This gives a theoretical upper temperature limit of 165°C. However, we are then right at the knee in the magnetization curve, we better subtract at least 20°C from this value, which gives a practical upper temperature limit of 140°C for baking the undulator vacuum system.

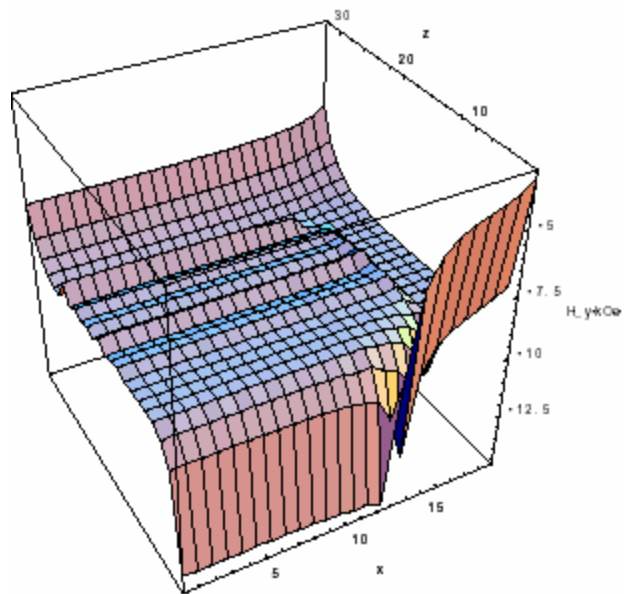


Figure 14. The de-magnetizing field in the (x,z) plane 0.1 mm inside the magnet block. The highest value, -14.5 kOe, is found where the pole ends. The structure visible is an artifact due to the pole subdivision.

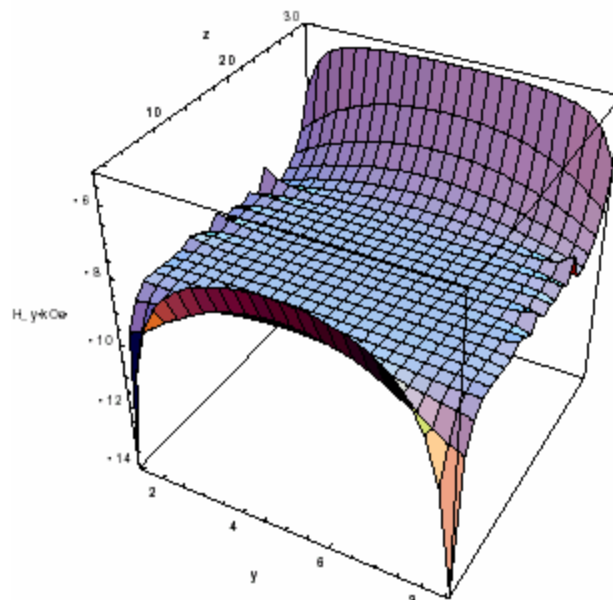


Figure 15. The de-magnetizing field in the (y,z) plane at $x = 0$ inside a magnet block. We see clearly the de-magnetizing field is largest at the corners close to the poles and the air gap.

3.5 EFFECTS ON THE STORED ELECTRON BEAM

Figure 5 shows a flux density distribution with a very flat top, and we do not expect any strong second order interaction between the stored electron beam and the undulator. The second order effect generates a tune shift, which depends on the position of the electron when it enters the undulator.

The tune shifts can be calculated from a potential of the form [5]

$$\Phi(x, z) = -\frac{1}{2} \left(\frac{e}{\gamma mc} \right)^2 \int_{-\infty}^{\infty} \left[\left(\int_{-\infty}^y B_x(x, z, y') dy' \right)^2 + \left(\int_{-\infty}^y B_z(x, z, y') dy' \right)^2 \right] dy$$

where e is the electron charge, γmc is the electron momentum, and B_x and B_z are the horizontal and vertical components of the magnetic flux density. The integrals can be solved analytically if we neglect the end sections and make a Fourier expansion of the magnetic flux density. B_x is zero, but B_z has strong 3rd and 5th components, which we include. The potential then takes the form

$$\Phi(x, z) = -\frac{L_u}{2} \left(\frac{ecI_u}{2pE_e} \right)^2 \left[B_1(x, z) + \frac{1}{3} B_3(x, z) + \frac{1}{5} B_5(x, z) \right]^2$$

where L_u is the length of the undulator, λ_u the undulator period length, E_e the electron beam energy and B_1 , B_3 and B_5 the amplitude of the $n = 1, 3$ and 5 components in the Fourier expansion. The potential is shown in Figure 16.

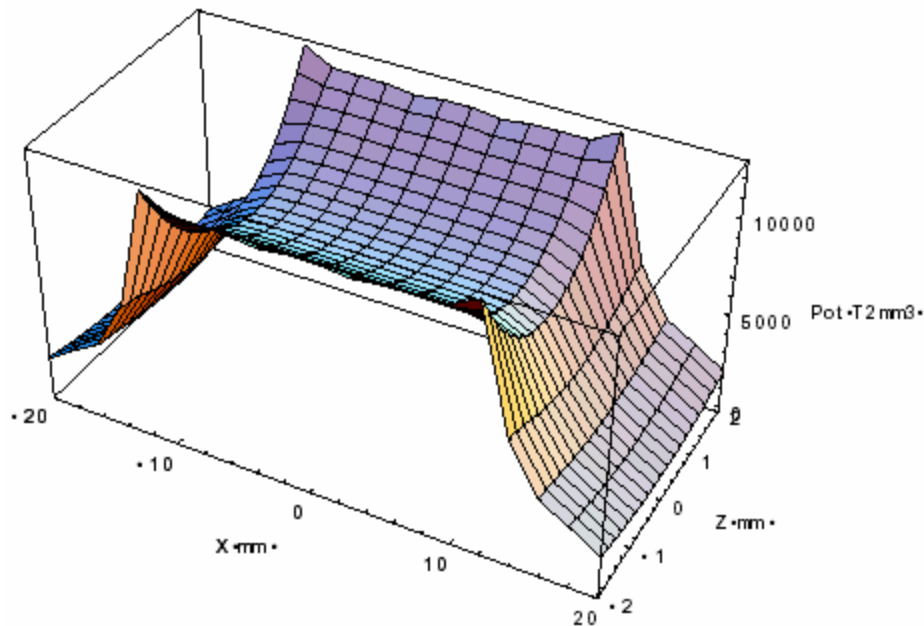


Figure 16. The second order focusing potential for the undulator at minimum gap using the three first terms in the Fourier expansion of the magnetic flux density.

The tune shifts are proportional to the second derivative of the potential

$$dn_x = \frac{b_x}{4p} \frac{\partial^2 \Phi}{\partial x^2}$$

$$dn_z = \frac{b_z}{4p} \frac{\partial^2 \Phi}{\partial z^2}$$

where β_x and β_z are the average horizontal and vertical beta functions for the straight section. The tune shifts are shown as functions of x on the magnetic mid plane for 5 mm gap in Figure 17. The tune shift decreases rapidly when the undulator gap is increased.

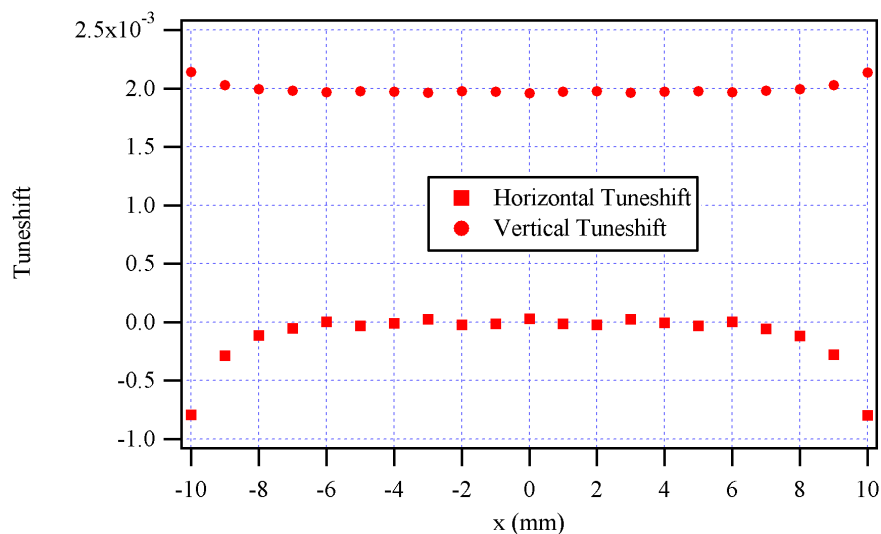


Figure 17. The dynamic tune shift on the magnetic mid plane.

As expected the horizontal tune shift is very small in the interval $-10 \text{ mm} < x < 10 \text{ mm}$. The vertical tune shift is constant 2×10^{-3} , caused by the cosh behavior of the magnetic flux density in the vertical direction.

3.6 PERMANENT MAGNET MATERIAL, MANUFACTURING AND QUALITY CONTROL.

The permanent magnet blocks will be manufactured by transverse die pressing. The blocks are produced individually by pressing powder in a die in presence of a polarizing field. The direction of the field is perpendicular to the pressing direction. The dimensions of the pressed blocks are close to the final ones reducing the machining, and the remanence is close to the maximum attainable. Transverse die pressed blocks have good homogeneity and are close to identical, which is a great help in the shimming process.

The blocks will be coated with TiN or Ni for HUV compatibility. Both have been used for in-vacuum undulators with good results. The poles will probably need a coating, a few μm of Ag is proposed, as it will lower the friction between the pole and the magnet blocks, which will be helpful in the shimming process.

We specify the block and pole dimensions and tolerances, both the dimensions and shape, for the uncoated poles and blocks. Furthermore we specify the lower limit on the remanence and the tolerance of the variation of the total magnetic dipole moment for the blocks. We also specify the tolerance on the variation of the direction of the easy axis for the blocks.

The manufacturer will check the dimensions of each pole and block before applying the anti-corrosion coating; the blocks are then non-magnetic. After the blocks have been coated and magnetized they are measured with a Helmholtz coil to check that they are within the tolerances on the total magnetic moment and the direction of the easy axis. Furthermore the manufacturer checks that the corners and edges of the blocks are not chipped.

After delivery to CLS the blocks will be visually inspected. The vertical and horizontal integrals of each block as function of x will be measured with the moving wire bench and stored in a database to be used in the shimming process.

In the assembly process we will use the Hall probe bench to assure the period length is uniform through the undulator and that the poles in the upper and lower magnet assemblies are directly above each other. Each time we have an asymmetric configuration we will measure the first integral as function of x and select blocks from the data base to eliminate the integrals, or, if we cannot find a suitable block, to apply shims. Thus the assembly and the multipole shimming take place at the same time.

We need up to the 11th harmonics to cover the specified photon range. To get less than a 10% reduction in the peak intensity at 11th harmonics we need a RMS phase angle error of about 1° at the end of the spectrum shimming.

3.7 MOUNTING OF THE MAGNET ASSEMBLIES

To get as large a maximum gap as possible inside the vacuum chamber we must mount the magnet assemblies directly on the girders without using assembly plates. The interface between the magnet assemblies and the girders can only be determined in the design stage of the undulator support structure.

3.8 CORRECTION COILS

Hybrid undulators pick up and amplify the earth's magnetic field and stray magnetic fields. The field integrals measured when the undulator is installed in the tunnel will probably be different from what has been measured in the insertion device laboratory. We need correction coils to correct the field integrals empirically using the stored electron beam and beam position monitors as measurement devices.

If we install two in-vacuum devices in the same straight, a long correction coil with vertical field will be installed on the outside of the vacuum chamber of each device. We can then use lacquer-insulated copper wire, which can be baked at high temperatures. We have chosen a symmetric layout for the undulator, and the long coil can correct both the vertical first and second integrals. There will be chicane magnets around each device, and they can be used to correct the vertical second integral if necessary.

Correction coils with horizontal field will be very inefficient if installed on the outside of the vacuum chamber, the field lines will be shunted through the iron poles instead of going through the air gap. The better places for the horizontal correction coils are around the bellows at the entrance and exit of the ID straight, and in the middle chicane magnet, where the air gap is much larger.

If extra quadrupoles are introduced to re-distribute the beta-functions in the straight section we can only install one undulator. In this case there will probably be place in front and behind the undulator to install short correction magnets with horizontal and vertical field.

3.9 SUMMARY

Photon Energy Range	6 – 18 keV
Undulator Type	Hybrid
Undulator Symmetry	Symmetric
Period Length	20 mm
Total Number of Poles	159
Number of Full Size Poles	157
Length of Magnet Assemblies	1583 mm
Total Length of Undulator	1607 mm
Minimum Gap	5 mm
Maximum Gap	To be determined
Operating Temperature	27°C
β Values for the CLS ID Straights:	
Horizontal	9.67 m
Vertical	2.46 m
Permanent Magnet Material	VACOMAX 225 HR
Minimum Remanence at 27°C	1.03 T
Average Remanence at 27°C	1.10 T
Temp. Coefficient for Remanence	-0.035%/°C
Minimum Intrinsic Coercivity at 20°C	20 kOe
Average Intrinsic Coercivity at 20°C	26 kOe
Temp. Coefficient for Intrinsic Coercivity	-0.19%/°C
Baking Temperature	140°C
Minimum Gap:	
Peak Flux Density	1.066 T
Fourier Expansion:	
1 st Harmonics	0.981 T
3 rd Harmonics	0.082 T
5 th Harmonics	0.004 T
7 th Harmonics	-0.001 T
Peak Effective Flux Density	0.981 T
Effective K	1.83
Higher Order Contributions	8.4%
Photon Energy	1.49 keV
Magnetic Force	9.5 kN
Remarks:	
	The total length of the undulator includes the end plates and the magic finger holders.
	The data for VACOMAX 225 HR is taken from the manufacturer's catalogue.

4.0 REFERENCES

- [1] P. Elleaume, O. Chubar, J. Chavanne, Computing 3D Magnetic Field for Insertion Devices, Contributed paper, PAC'97, Vancouver.
- [2] Les Dallin, Technical Report 5.2.69.2 Rev. 2, CLS Main Ring Lattice, October 16, 2002.
- [3] O. Chubar, P. Elleaume, Accurate and Efficient Computation of Synchrotron Radiation in the Near Field Region, Contributed paper, EPAC'98, Stockholm.
- [4] J. Chavanne, P. Elleaume, P. van Vaerenbergh, Segmented High Quality Undulators, Contributed paper, PAC'95, Dallas.
- [5] P. Elleaume, A New Approach to the Electron Beam Dynamics in Undulators and Wigglers, Contributed paper, EPAC'92, Berlin.